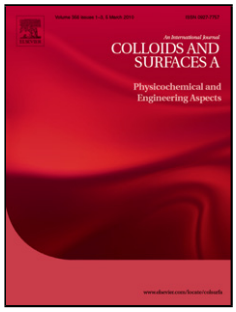

Title: A novel drug delivery system functionalized with K237 peptide for dual-responsive paclitaxel release and enhanced antitumor effect on MDA-MB-231 cells

Authors: Qianqian Qian, Shiwei Niu, Gareth R. Williams, Jianrong Wu, Xueyi Zhang, Li-Min Zhu

PII: S0927-7757(18)31519-X
DOI: https://doi.org/10.1016/j.colsurfa.2018.12.026
Reference: COLSUA 23065

To appear in: *Colloids and Surfaces A: Physicochem. Eng. Aspects*

Received date: 19 October 2018
Revised date: 10 December 2018
Accepted date: 12 December 2018

Please cite this article as: Qian Q, Niu S, Williams GR, Wu J, Zhang X, Zhu L-Min, A novel drug delivery system functionalized with K237 peptide for dual-responsive paclitaxel release and enhanced antitumor effect on MDA-MB-231 cells, *Colloids and Surfaces A: Physicochemical and Engineering Aspects* (2018), https://doi.org/10.1016/j.colsurfa.2018.12.026

A novel drug delivery system functionalized with K237 peptide for dual-responsive paclitaxel release and enhanced antitumor effect on MDA-MB-231 cells

Qianqian Qian[a, 1], Shiwei Niu[a, 1], Gareth R. Williams[b], Jianrong Wu[a], Xueyi Zhang[a], Li-Min Zhu[a,*]

[a]College of Chemistry, Chemical Engineering and Biotechnology, Donghua University，Shanghai, 201620, China

[b]UCL School of Pharmacy, 29-39 Brunswick Square, London, WC1N 1AX, UK

* Corresponding author.

E-mail: lzhu@dhu.edu.cn (L.-M. Zhu) , Tel：+862167792655 (L.-M. Zhu);

[1] These authors contributed equally.

Graphical abstract

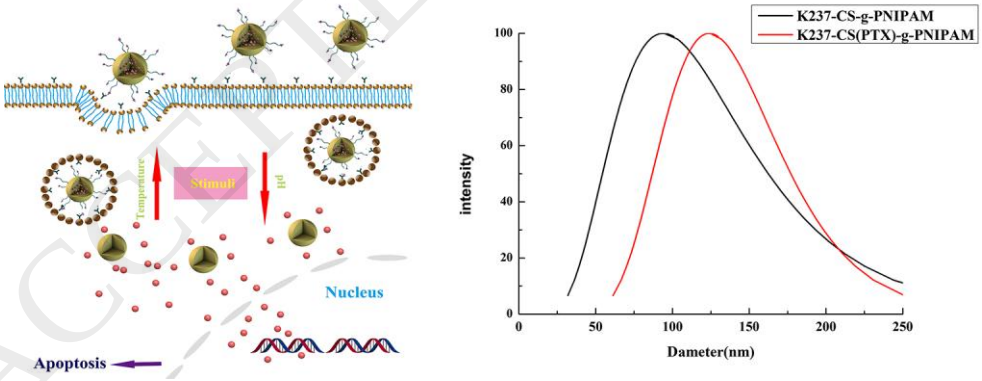

Highlights

- A novel peptide functionalized dual-responsive nanoparticles were synthesized successfully.
- The peptide binds to the KDR / Flk-1 tyrosine kinase, a key receptor which are overexpressed in tumor angiogenesis.
- Paclitaxel (PTX), a chemotherapy drug, was loaded into the nanoparticles.

- These drug loaded nanoparticles showed smart stimuli-responsive PTX release profiles.
- The peptide modified nanoparticles could precisely target KDR/Flk-1 overexpressing MDA-MB-231 human breast cancer cells, resulting in high levels of cytotoxicity.

Abstract:

In this work, we report K237-peptide functionalized chitosan (CS) nanoparticles (NPs) loaded with paclitaxel (PTX), for active targeting and effective treatment of KDR/Flk-1-overexpressing human breast cancer. The results displayed that the peptide-functionalized NPs put up favorable pH and temperature-sensitive characteristics. MTT assays showed that K237-CS (PTX)-g-PNIPAM NPs had a more peculiar and effective breast cancer cell growth inhibition compared with peptide-free NPs. Confocal experiments showed that the NPs could precisely target MDA-MB-231 human breast cancer cells which were over-expressing KDR/Flk-1 and could be effectively internalized into MDA-MB-231 cells, which verified that the uptake of FITC-K237-CS (PTX)-g-PNIPAM NPs was associated with KDR/Flk-1 on the breast cancer cell. These results indicate that the peptide functionalized NPs have potential applications for targeted delivery and the controlled release of anticancer drugs.

Key words: K237-peptide; dual-responsive; nanoparticles; targeted delivery; human breast cancer

1. Introduction

Breast cancer is one of the most common dangers to women's health. It is most commonly treated using chemotherapy [1] , but the active ingredients used in this are distributed systemically, leading to many side effects. Chemotherapeutic drugs are toxic to both cancerous and healthy cells, and cause numerous reactions such as hair loss, liver and kidney failure [2]. Paclitaxel (PTX) is often used for chemotherapy [3] , but also has poor specificity and an intrinsically low targeting capacity [4]. In the clinical, PTX leads to a series of side effects, and its applications are dramatically limited owing to its poor aqueous solubility. In order to increase the efficacy of clinical treatments for breast cancer [5, 6], nanoscale-formulations have been the focal point of many studies seeking to increase the solubility and applied range of PTX [7, 8]. There are numerous approaches that may be taken in developing new drug delivery systems, but one which has attracted a lot of attention is the production of targeted carriers [9].

These can have high specificity, allowing them to avoid damage to normal tissues. Nanoscale formulations can be selectively taken up by cancerous tissues or cells by the EPR effect, giving them a passive targeting functionality [10-12].

It is well known that there are significant differences between the microenvironment of tumoral tissue and that of normal healthy tissue. The tumor tissue's blood vessels are dilated and bent, and the lack of lymphatic flow causes the pressure inside the tumor tissue to be significantly higher than the surrounding tissues. Because the tumor cells multiply uncontrollably, and as a result of the anaerobic and acidic pH environment of the tumor, the temperature is higher than normal tissues [13, 14]. This offers a number of opportunities to deliver a drug payload selectively to cancer cells.

Recently, much research has focused on the preparation of stimuli-responsive polymers in order to obtain materials able to respond to specific changes in physiological conditions [15]. These can be pH and temperature-sensitive (or both), and are commonly termed ‘smart polymers’ [16]. For instance, thermosensitive variants of chitosan (CS) can be prepared through its reaction with poly(N-isopropylacrylamide) (PNIPAM) [17, 18]. CS has been extensively studied, and chitosan nanoparticles (CS NPs) in particular have great promise as drug delivery materials [19, 20]. CS is sensitive to pH, and thus has the potential to permit targeting to the low-pH environment of the tumor. PNIPAM is a widely explored thermally responsive polymer which undergoes a hydrophilic-to-hydrophobic phase transition in water at 32 ºC [21, 22] . This can be exploited in the biomedical field to control drug release. In addition, PNIPAM is biodegradable. Therefore, PNIPAM grafted CS materials have on several occasions been synthesized as dual-responsive systems in the biomedical domain [23, 24]. In this study, we synthesized CS-g-PNIPAM NPs using the RAFT technique [25]. However, although this provides for the formulation to respond to both temperature and pH, for effective cancer therapy the specificity of the nanoparticles toward tumors requires further improvement [26].

To further improve their specificity for tumors, active targeting strategies have been developed applying functional targeting moieties to bind cell-specific surface markers, which are overexpressed on the surface of different cancer cells. These targeting moieties can be some proteins, peptides, RNA, or other biomolecules [27-29]. These targeting ligands are used to functionalize the NPs to distinguish and have a strong binding affinity to tumor cells, selective targeting can be achieved. This allows the loaded drug to be delivered specifically to the tumor site, resulting in active targeting at the cellular level [30, 31]. Peptide ligands are particularly promising as active targeting ligands; suitable molecules

are commonly discovered by selection from a random peptide library using display technologies, or from the sequences of the binding proteins [32, 33].

Niu *et al.* [16] of our group reported a dual-responsive nanomaterial based on chitosan for breast tumor therapy before, it's notable that, the recognition of this nanomedicine is depend on the guiding property of L-peptide, which can bind to glucose-regulated protein 78 (a verified specific tumor surface marker, and ubiquitously presented on various kinds of carcinomas). Although, the well fabricated nanomedicine acquired a favorable therapeutic effect on breast tumor, there are still some drawbacks, which hindered the effective and targeting therapeutic effect in depth. Here, we employed a 12-mer peptide which was isolated from a phage display library [34]. This K237 peptide (HTMYYHHYQHHL-NH_2) binds to the KDR/Flk-1 tyrosine kinase, one of two key receptors for vascular endothelial growth factor which are overexpressed in tumor angiogenesis. In addition, it is reported that L-peptides might bind GRP78 (glucose-regulated protein 78), a verified specific tumor surface marker. Obviously, the composition and length for these two peptides were different, especially different targeting sites for the two peptides to bind. K237 peptides have been reported to disrupt the angiogenic mimicry channels formed by tumor cells [34]. Thus, this versatile peptide might serve as an ideal ligand for tumor vessel targeting [35]. To improve their tumor-selective targeting effects, the K237-peptide was hence used to functionalize the CS-g-PNIPAM NPs endowing them with both passive and active targeting properties. The formulation was finally loaded with PTX [36, 37], before being explored for breast cancer applications. Moreover, we replaced the former high molecular weight chitosan with a low molecular weight chitosan, in this way, we obtained a type of updated nano-scale material with optimal size (100 nm), to exhibit the better EPR effect. The strategy underlying this work is depicted in Scheme 1. The stimuli-responsive behavior of the NPs, their drug release behavior, cytotoxicity and capacity to target cancer cells were all examined in detail [38, 39]. Our results showed specific tumor targeting and potent antitumor activity, suggesting that K237-CS-g-PNIPAM NPs may be useful for antitumor drug delivery applications.

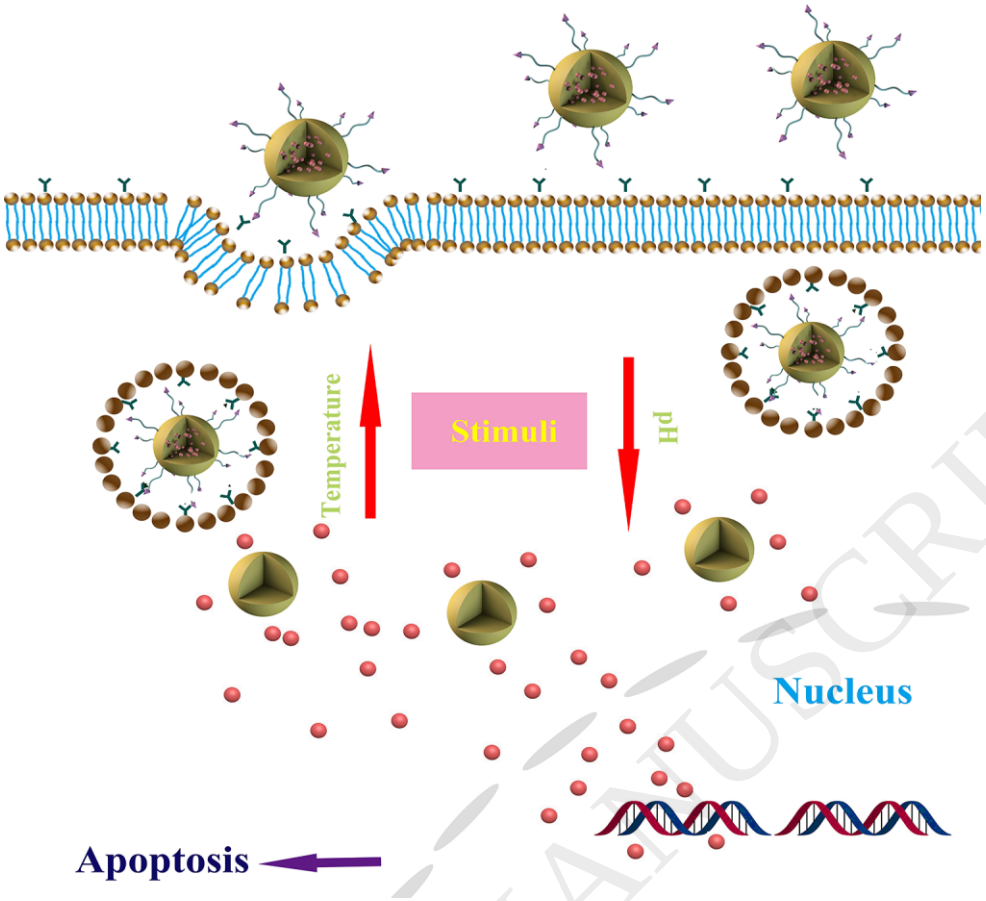

Scheme1 The illustration of the temperature-and pH-responsive K237-CS (PTX)-g-PNIPAM NPs for active KDR/Flk-1 targeted PTX delivery.

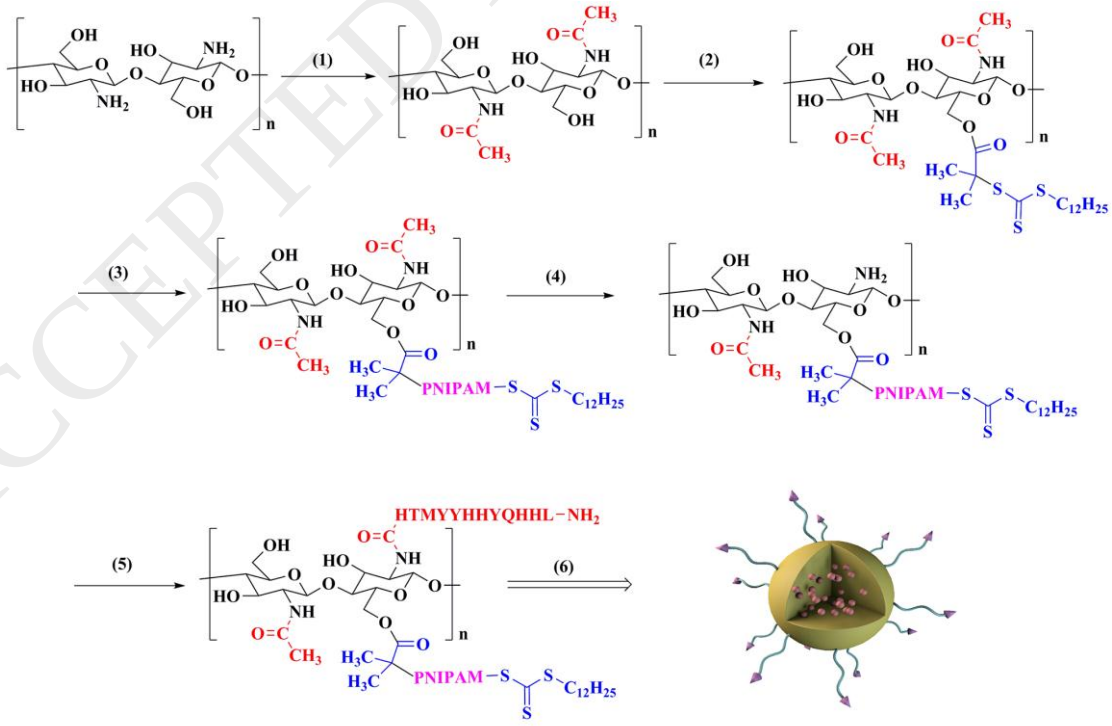

Fig. 1 The synthesis of K237-CS (PTX)-g-PNIPAM NPs. (1) Acetic anhydride, rt,4h; (2) DDACT,

DCC, DMAP, rt, 48 h; (3) NIPAM, AIBN, 60 ºC ,48h; (4) Hydrolysis, rt; (5) K237 peptide, EDC, NHS; (6) PTX, self-assembly.

2. Experimental

2.1. Materials

CS (degree of deacetylation > 95%) and acetic anhydride (analytical grade) were obtained from the Sinopharm Chemical Reagent Co, Ltd (China). *N*, *N*-dimethylformamide (DMF), dimethyl sulfoxide (DMSO), dicyclohexylcarbodiimide (DCC), 4-(*N*,*N*-dimethylamino) pyridine (DMAP), S-1-Dodecyl-S'-(α, α'-dimethyl-α''-acetic acid) trithiocarbonate (DDACT), *N*-isopropylacrylamide (NIPAM), azobisisobutyronitrile (AIBN), *N*-hydroxysuccinimide (NHS; analytical grade), PTX, acetic acid, methanol, ethyl ether, acetone, fluorescein isothiocyanate (FITC), and 3-(4, 5-dimethyl-thiazol-yl)-2, 5-diphenyltetrazolium bromide (MTT) were procured from Sigma-Aldrich (USA). *N*-(3-dimethyl-aminopropyl)-*N*'-ethylcarbodiimide hydrochloride (EDC) was obtained from Shanghai Titan Polytron Technologies Inc (China). The K237 peptide was supplied by GL Ltd (China).

L929 cells and MDA-MB-231 cells were sourced from the Type Culture Collection of the Chinese Academy of Sciences (China). Fetal bovine serum (FBS), RPMI 1640 and DMEM media, and dialysis bags were obtained from the Sinopharm Chemical Reagent Co, Ltd (China). All other reagents were sourced from Meryer Chemical Technology Co, Ltd (China).

2.2. Synthesis of CS-based RAFT agent

The preparation of the functional NPs generated in this work was based on the RAFT method (Fig. 1). The CS-based RAFT agent was synthesized according to a previous report [40]. Firstly, 5 g of CS was dissolved in 250 mL glacial acetic acid (1.0 %, w/v) with acetic anhydride at a molar ratio of 5:1. This step was undertaken to protect the NH_2 group of CS. After addition of 250 mL absolute ethanol, the mixture was reacted for 4 h to obtain *N*-acetyl CS. The acetylated CS (0.298 g) was dissolved in anhydrous DMF (30 mL) under stirring, then 0.370g DDACT, 0.205g DCC, and 0.015g DMAP were added and the reaction allowed to proceed at room temperature for 48 h with continuous stirring. The resulting solution was poured onto ice water. The precipitate was collected on a filter, washed with acetone by Soxhlet's extraction, and dried to give a yellow powder.

2.3. Preparation of CS-g-PNIPAM

A mixture of the CS-RAFT agent (0.0468 g) and anhydrous DMF (5 mL) was stirred magnetically under a nitrogen atmosphere. Once the CS-RAFT powder had dissolved completely, AIBN (0.0016 g, 0.01 mmol) and NIPAM (0.50 g) were added. Polymerization was undertaken at 60 ºC for 24 h under a

nitrogen atmosphere. Subsequently, the reaction mixture was precipitated in 10-fold diethyl ether, and finally the precipitate was filtered to obtain *N*-acetyl CS-g-PNIPAM.

2.4. Synthesis and purification of K237-CS-g-PNIPAM

Acetyl groups were removed by agitating the *N*-acetyl CS-g-PNIPAM in NaOH solution (14.2 M) for two days at room temperature. Next, the K237 peptide solution (30 ppm) was mixed with CS-g-PNIPAM (20 mg) in DMSO (15 mL) at 4 °C [41]. EDC (20 mg) and NHS (16 mg) were then added to the mixture and stirred for 24 h at 4 °C to avoid denaturing the K237 peptide. The reaction mixture was then dialyzed against an aqueous 1.0 mM NaOH solution using a 1000 Da MWCO membrane for 72 h. Finally, the dialyzed product was lyophilized to yield the graft copolymer K237-CS-g-PNIPAM.

2.5. Characterization

^{1}H NMR spectra was obtained in DMSO-d6 using a DRX 400 nuclear magnetic resonance spectrometer (Bruker, Germany). Fourier transform infrared (FTIR) spectra were recorded on a Nicolet Nexus 870 spectrometer (Nicolet Instruments Inc., USA) over the range 4000–500 cm^{-1} and with a resolution of 2 cm^{-1}. The morphology of the CS NPs was examined via transmission electron microscope (TEM; JEM-2100, JEOL, Japan). Thermogravimetric analysis (TGA) was performed using a Q500 TGA (TA instruments, UK). The samples heated at 20 ºC min^{-1} to 900 ºC in air. Zeta potentials were quantified on a Nano ZS system (Malvern Instruments, UK). Dynamic light scattering (DLS) was performed with a BI-200SM instrument (Brookhaven, USA). UV-vis absorption spectra spectra were recorded on a UV3600 UV-Vis-NIR spectrophotometer (Japan).

2.6. PTX loading

For the preparation of PTX loaded NPs (CS (PTX)-g-PNIPAM or K237-CS (PTX)-g-PNIPAM NPs), following the methods described in a previous report PTX (5 mg) and modified CS NPs (25 mg) were dispersed in DMF (5 mL). The mixture was agitated for 24 h at 25 ºC. The products were collected by centrifugation (11,000 rpm, 30 min) to get rid of unencapsulated drug [42]. The drug loading efficiency (LE) was calculated by means of measuring the dose of PTX in the supernatant. PTX was quantified by HPLC with UV detection at 227 nm, using acetonitrile/water (1/1, v/v) as a mobile phase. The LE was calculated with reference to a predetermined PTX calibration curve using the formula:

LE = (total mass of PTX — mass of PTX in the supernatant)/total mass of PTX-loaded NPs ×100%.

2.7. PTX release

In addition, the release behaviour of PTX from PTX loaded NPs was carried out at different pH and different temperature in a dialysis bag (MWCO 3500 Da). The K237-CS (PTX)-g-PNIPAM NPs (1.0 mg) added in PBS (2.0 mL, pH 7.4) or acetate buffer (2.0 mL, pH 5.0) was then put in the same buffer medium[43]. At set time intervals, a simple of 1 mL was withdrawn from the release medium. The dose of PTX released examined by HPLC measurement. Simultaneously, 1 mL of equal volume of fresh media was replenished into the release medium to maintain the volume constant. Analogous experiments were carried out at 25°C and 37°C respectively to probe the effect of different temperature on PTX release [44, 45]. PTX release experiments were performed five times, and the results are reported as mean ± SD.

2.8. Cell viability

The cytotoxicity of K237-CS-g-PNIAPM NPs was evaluated using MDA-MB-231 breast cancer cells which express KDR / Flk-1 receptors. L929 cells which not express KDR / Flk-1 receptors were as control. In brief, each cell line was plated in a 96-well plate using DMEM medium supplemented with 10% fetal bovine serum, penicillin (100 U/mL), and streptomycin (100 mg/mL). The cells were seeded at a density of 1×10^4 cells/well. After 24h, 20 µL of a PTX solution (giving final concentrations ranging from 0.001 to 10 µg/mL) or a PBS suspension of the PTX-loaded NPs (CS (PTX)-g-PNIPAM and K237-CS (PTX)-g-PNIPAM) containing equivalent PTX concentrations was added to each well. After incubation for another 24 h, 20 µL of MTT solution (0.5 % w/v) was added and the plate incubated for an additional 4 h. The liquid in each well was then removed, replaced with 200 µL DMSO, and the plate shaken for 15 min. Afterwards, the absorbance was measured at a wavelength of 450 nm on a microplate reader Multiskan FC, Thermo Scientific, USA). Control cytotoxicity experiments were also performed on the blank K237-CS-g-PNIPAM and CS-g-PNIPAM NPs (with no PTX loaded) at the same carrier concentrations. The experiments were performed in triplicate.

2.9. Preparation of FITC labeled NPs and Cellular uptake evaluation

In order to evaluate of the cellular uptake of the NPs, K237–CS(PTX)-g-PNIPAM and CS(PTX)-g-PNPAM were firstly labeled with FITC. These fluorescent NPs (denoted FITC-CS(PTX)-g-PNIPAM and FITC-K237-CS(PTX)-g-PNIPAM) were synthesized according to a previously report [4]. Briefly,

FITC (10 mg) was dissolved in ethanol (5 mL), then added to CS(PTX)-g-PNIPAM or K237-CS(PTX)-g-PNIPAM NPs aqueous suspensions (6 mg/mL, 5 mL). The mixture was stirred in the dark for 8 h at room temperature. Subsequently, the suspension (10 mL) was dialyzed against 100 mL of ultrapure water in the dark to remove unreacted FITC. The dialysis medium was replaced three times a day until no fluorescence was detected in the supernatant.

The cellular uptake of the NPs by L929 and MDA-MB-231 cells was explored through confocal microscopy. The cells were cultured in a 24-well plate (2×10^4 cells/well) in DMEM medium supplemented with 10% fetal bovine serum, penicillin (100 U/mL), and streptomycin (100 mg/mL). After 24 h, FITC-CS(PTX)-g-PNIPAM NPs or FITC-K237-CS(PTX)-g-PNIPAM NPs (0.5 mg/mL) in 2 mL was added to each well. After incubation for 2 h, the culture medium was removed and the cells were washed three times with PBS. Next, the cells were fixed with glutaraldehyde (2.5% v/v in PBS) for 15 min at 4 ºC before being stained with Hoechst 33342 (1 μg/mL) for 20 min [46-48]. Finally, the cells were imaged with a confocal laser-scanning microscope (LSM 700 instrument, Carl Zeiss, Germany). The confocal experiments were repeated three times.

2.10. Statistical analysis

One-way analysis of variance (ANOVA) statistical method was performed to evaluate the experimental data. All experiments were repeated at least three times, and the data are displayed as mean ± standard deviation (SD).

3. Results and discussion

3.1. Synthesis and characterization of modified CS

The preparation of the peptide functionalized dual-responsive CS NPs K237-CS-g-PNIPAM anticancer drug-carrier is presented in Fig. 1. First, the CS-g-PNIPAM copolymer was synthesized by graft polymerization of NIPAM onto CS. The K237 peptide was then conjugated onto CS-g-PNIPAM using the EDC-NHS technique. The formation of copolymers was confirmed by FTIR and ^{1}H NMR. The ^{1}H NMR spectrum of CS-g-PNIPAM is shown in Fig. S1 (Supporting Information) and that of K237-CS-g-PNIPAM NPs in Fig. 2. Considering first CS-g-PNIPAM (Figure S1), protons on the DDACT segment of the RAFT reagent appear at δ = 1.20 ppm. The peak at 3.3 ppm corresponds to CS. At δ = 1.00 ppm, protons on the t-butyl and methyl groups of DDACT can be seen. Characteristic peaks of NIPAM are present at δ = 3.90 ppm and 0.82 - 2.10 ppm. These observations, plus the lack of

vinyl protons in the spectrum, verify the existence of CS and PNIPAM in the copolymer. K237 was then grafted onto CS-g-PNIPAM by reaction between amino and carboxyl groups under EDC-NHS catalysis. In Fig. 2, in addition to the aforementioned peaks from CS and PNIPAM, the characteristic resonances of K237 are shown at 7-9 ppm in K237-CS-g-PNIPAM, demonstrating successful functionalization.

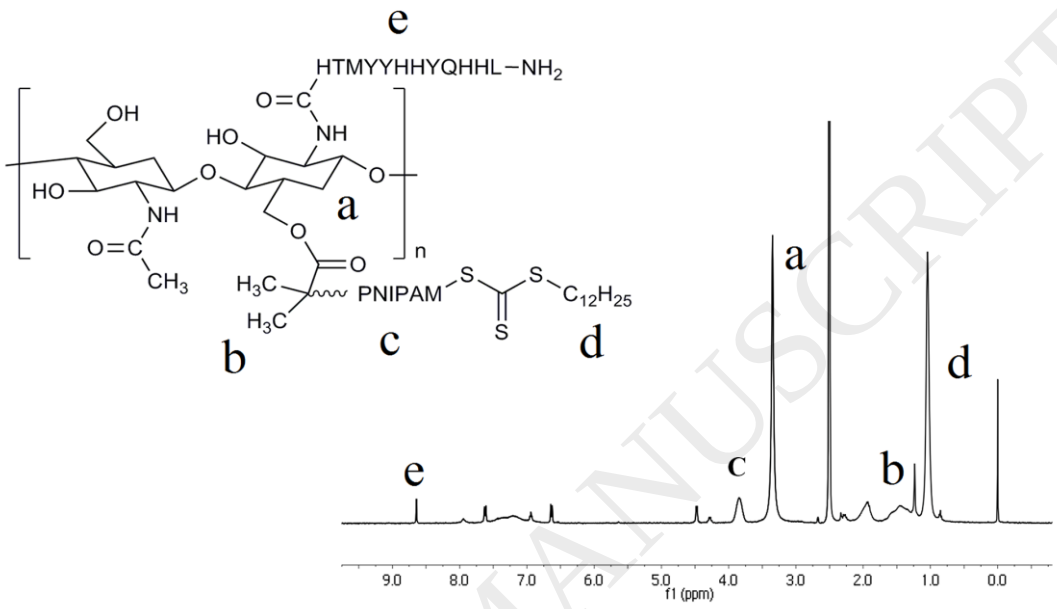

Fig. 2 The ^{1}H NMR spectrum of K237-CS-g-PNIPAM NPs. The resonance at 2.5 ppm is the DMSO solvent peak.

The modified CS materials were further characterized by FT-IR spectroscopy, and the spectra obtained for CS, *N*-acetyl CS, CS-RAFT and CS-*g*-PNIPAM is given in Fig. 3. When CS is modified with acetic anhydride, the characteristic peak of CS at 1642 cm^{-1} is reduced in intensity. This is because in *N*-acetyl CS, the acetyl group has replaced some of the NH_2 groups of CS. The CS RAFT agent has an additional feature at around 1720 cm^{-1} (C=O) which arises from DDACT. The C-H stretching bands at 2800 ~ 3000cm^{-1} are also enhanced in CS-RAFT, due to the methyl group and methylene groups of DDACT. A peak at 1520 cm^{-1} can be attributed to the vibration of the -SC=S bond of DDACT. This indicates that DDACT has reacted with acetylated CS successfully, and the hydroxyl groups of acetylated CS were replaced with DDACT. Characteristic peaks for CS-g-PNIPAM can be seen at 1460 cm^{-1} and 1645 cm^{-1}, corresponding to -CH_3 and C=O vibrations of PNIPAM. This verifies the presence of PNIPAM in the material. In addition, the band centered at 3310 cm^{-1} becomes broader compared to the RAFT material, indicating the formation of hydrogen bonds between -OH and -CONH groups. These results further demonstrate the successful synthesis of CS-*g*-PNIPAM.

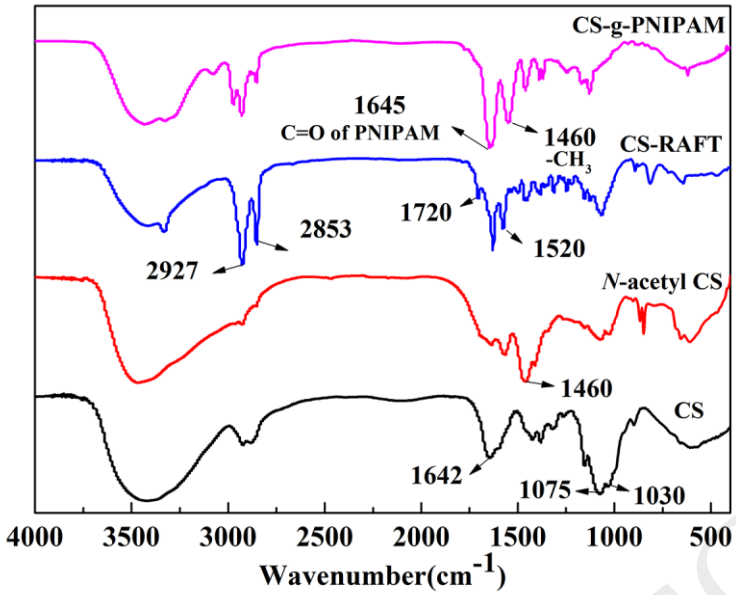

Fig. 3 FTIR spectra of CS, *N*-acetyl CS, CS-RAFT and CS-g-PNIPAM.

Zeta potential measurements were also obtained to verify the modification of CS (Table 1). The zeta potential of pure CS is positive (30.8 ± 1.6 mV) because it contains many amine groups. When CS is modified with acetic anhydride, acetyl groups replace some of the amines, so the zeta potential becomes less positive (*N*-acetyl CS: 17.7 ± 2.4 mV). Further, after reaction with DDACT and NIPAM, a number of acidic groups were added to the system, thus reducing the potential CS-g-PNIPAM further (to 14.1 ± 2.1 mV). The zeta potential of K237-CS-g-PNIPAM is more positive than the zeta potential of CS-g-PNIPAM, which is consistent with the presence of additional -NH_2 groups from the K237 peptide.

Table 1

Zeta potential values for the modified CS materials. Measurements were recorded three times and are reported as mean ± SD

	CS	*N*-acetyl CS	CS-RAFT	CS-g-PNIPAM	K237-CS-g-PNIPAM
Zeta potential (mV)	**30.8 ± 1.6**	**17.7 ± 2.4**	**15.4 ± 1.3**	**14.1 ± 2.1**	**19.1 ± 2.5**

TGA was performed to determine the compositions and thermal stability of the NPs. The TGA results for CS, CS-RAFT, CS-g-PNIPAM and K237-CS-g-PNIPAM are shown in Fig. 4a. The residual masses at 900 °C of CS, CS-RAFT, CS-g-PNIPAM and K237-CS-g-PNIPAM were 35%, 3%, 12% and 10%, respectively. Based on these data, we can calculate that the mass percentages of the grafted

DDACT and NIPAM in CS-g-PNIPAM are around 3% and 63%. In K237-CS-g-PNIPAM, the mass content of the grafted K237 is 5%, based on calculations described in the literature [39].

PNIPAM is a widely explored thermosensitive polymer with a marked hydrophilic to hydrophobic phase transition (termed the lower critical solution temperature, LCST) at around 32 ºC. This can easily be quantified through the absorbance of the material (Fig. 4b). The absorbance of CS-g-PNIPAM NPs in aquous solution at 500 nm as a function of temperature was measured by UV3600 spectrophotometer. CS-g-PNIPAM has a significant phase transition at around 25 ~ 34 ºC, with an LCST of 32 ºC. This proves that the polymer prepared has good thermosensitivity.

The morphology of the K237-CS-g-PNIAM and K237-CS (PTX)-g-PNIAM NPs was examined by TEM. The TEM images of the NPs isolated from dilute dispersions in water at room temperature are shown in Fig. S2 and 4c. The K237-CS-g-PNIAM copolymer self-assembles in water to form roughly spherical shaped particles with diameters around 100 nm (Fig. S2). After loading of PTX, the diameter of NPs expanded. But their spherical shapes remain unchanged (Fig. 4c). The size distributions measured by DLS are relatively narrow (PDI range 0.1 – 0.3), with the K237-CS(PTX)-g-PNIAM NPs being around 125 nm in size (Fig. 4d). This is suitable for cellular uptake and tumor targeting, allowing potential intravenous administration [16].

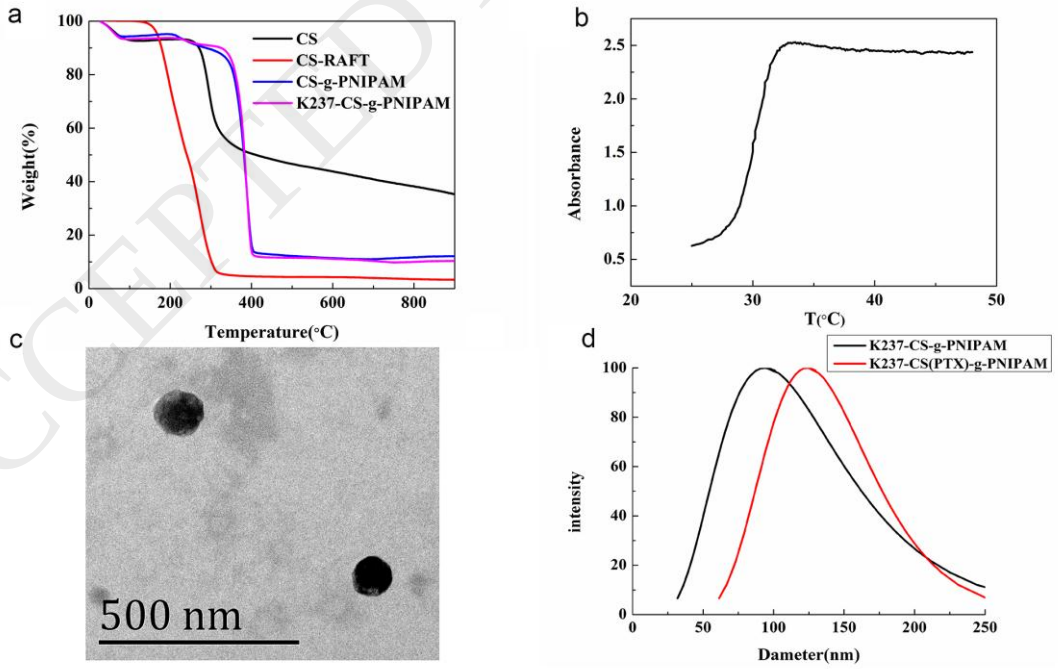

Fig. 4 a TGA curves of CS, CS-RAFT, CS-g-PNIPAM and K237-CS-g-PNIPAM; **b** The absorbance at

500 nm of CS-g-PNIPAM as a function of temperature; **c** TEM image of K237-CS(PTX)-g-PNIPAM NPs and **d** DLS data for K237-CS(PTX)-g-PNIPAM and K237-CS-g-PNIPAM NPs**.**

3.2. PTX loading and release

The K237–CS-g-PNIPAM copolymer is amphiphilic and can thus self-assemble into NPs in an aqueous medium. In this structure, the presence of zwitterionic PNIPAM at the surface can prevent aggregation, and PTX can be loaded into the hydrophobic CS core via physical incorporation [41]. The drug loaded NPs were isolated by ultracentrifugation and the LE was computed by means of measuring the dose of PTX in the upper layer by HPLC. The LE of K237-CS (PTX)-g-PNIAM NPs was found to be around 11.8%.The influence of environmental conditions on the release of PTX from PTX loaded NPs was studied at two different temperatures and pH. As expected, both pH and temperature influenced the release of PTX from K237-CS (PTX)-g-PNIPAM (Fig. 5). In *vitro* release studies at 37 ºC showed that drug release from K237-CS (PTX)-g-PNIPAM was highly dependent on pH, with 63% and 74% of the incorporated PTX released after 48 h at pH 7.4 and pH 5.0, respectively. When the temperature decreased to 25 ℃, the release rate significantly decreased and only 39% of the PTX content was released at pH 7.4 release system after 48 hours. At pH 5.0, a greater amount of PTX (57 %) was freed into solution, but again this is less than at 37 °C. This behavior may be attributed to the phase transition of the PNIPAM. After 72 hours, a total of ca. 65% and 41% of the total PTX was released at 37 ºC and 25 ºC and pH 7.4. Similarly, at pH 5.0 the total release of PTX at 37 ºC is much greater than at 25 ºC. Overall, faster release rates were observed when the drug-loaded NPs were in milieu at higher temperature and lower pH values. These results indicate that K237-CS-g-PNIPAM NPs could lead to selective drug accumulation in tumors, and avoiding harmful side effects in normal tissues.

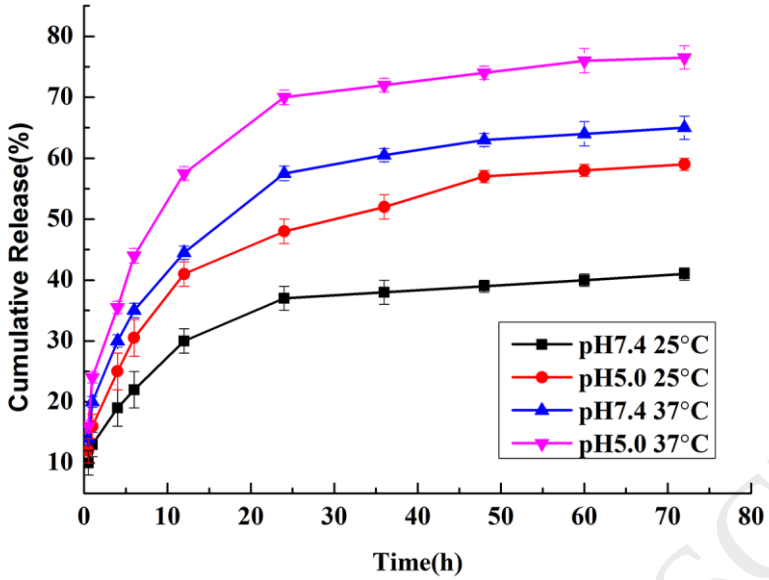

Fig. 5 The release of PTX at different pH and temperature as measured using a dialysis method. Data are reported as mean ± SD from five independent experiments.

3.3. Model Fitting

Studies have shown that the kinetics of drug release can be modeled using equations such as zero-order equations, first-order equations, Higuchi and Hixson-Crowell's [49, 50]. The pH of the medium largely affects the release rate of macromolecular drugs. Many of the original drugs used in macromolecular drugs are acidic. In order to simulate different body fluid environments *in vivo*, this experiment selected the effect of two different pH values on drug release. The Release kinetics of PTX from K237-CS (PTX)-g-PNIPAM in different pH at 37°C were shown in table 2 below. As shown in Figure 5, the drug release rate under acidic conditions is much higher than the release rate under neutral strips. Within 48 h, the cumulative release of PTX reached 74% at pH 5.0, while the cumulative release of the drug at pH 7.4 was only 63%. Chitosan is pH sensitive, and macromolecules have a greater degree of swelling under acidic conditions, releasing drugs quickly. From the R^2 value in Table 2, it can be seen that the release profile of the drug under acidic conditions is in accordance with the Weibull kinetic equation, and the pH 7.4 is more consistent with the Ritger-Peppas kinetic model.

Table 2

Release kinetics of PTX from K237-CS (PTX)-g-PNIPAM in different pH at 37°C

Release	Ritger-Peppas	Weibull	Higuchi

duration	$K_{RP} \times 10^4$ ((ln min)$^{-1}$)	R^2	$K_W \times 10^4$ ((lg min)$^{-1}$)	R^2	$K_H \times 10^4$ (min$^{-1/2}$)	R^2
5.0	0.4572	0.94973	0.4621	0.99086	19.4	0.99058
7.4	0.8704	0.97876	0.88524	0.97796	52	0.9676

It is well known that an increase in temperature tends to result in an increase in the diffusion of molecules in a liquid or solid, which has a significant effect on drug release. This experiment investigated the drug release behavior of the drug at different temperatures (25, 37 °C). At pH 7.4, the release profile at different temperatures is shown in Figure 5. When the temperature dropped to 25 °C, the rate of release was significantly reduced, and after 48 hours, only 39% of the amount of PTX was released in the pH 7.4 release system. This result indicates that the *in vitro* release of the drug increases with increasing temperature. This phenomenon may be due that PNIPAM is a widely explored thermally responsive polymer. The low critical solution temperature (LCST) of PNIPAM is closer to body temperature. When the heating temperature exceeds 32°C, it can undergo a phase change in water and increase the drug release rate. Table 3 is the kinetic data after fitting to various kinetic models. By analyzing the correlation coefficient R^2 of the release curve fitting, it can be found that the two temperatures are in line with the first-order kinetics. The correlation coefficients are 0.98904 and 0.97804, respectively. Increased temperature accelerates drug release.

Table 3

Release kinetics of PTX from K237-CS (PTX)-g-PNIPAM at different temperature in PH 7.4

Release duration	Zero-order		First-order		Higuchi	
	K_0(min^{-1}) $\times 10^4$	R^2	K_1 (min $^{-1}$) $\times 10^4$	R^2	K_H (min$^{-1/2}$) $\times 10^4$	R^2
25 ºC	0.25929	0.98862	-0.26244	0.98904	7.8104	0.97288
37 ºC	1.6942	0.97525	-1.8016	0.97804	52	0.9676

3.4. Cell cytotoxicity and cell uptake

The cytotoxicity of the drug-loaded NPs was quantified in order to determine their influence on different cell types. The results of MTT assays on L929 cells and MDA-MB-231 cells are shown in Fig. 6. Both CS–g-PNIPAM and K237-CS–g-PNIPAM lead to generally high cell viabilities of >90%

with both cell types, indicating their biocompatibility as drug carriers.

Considering the L929 (non-cancerous, KDR/Flk-1 negative), it can be seen that there is a decline in viability with increasing PTX dose, with viability at around 70% with the highest dose of 10 µg/mL. The PTX-loaded formulations result in a smaller decline in viability, with both K237-CS(PTX)-g-PNIPAM and CS(PTX)-g-PNIPAM giving viability of ca. 80% at an equivalent PTX dose of 10 µg/mL. The MDA-MB-231 cells are cancerous and KDR/Flk-1 positive, and a stark difference in the viability trends are seen. Free PTX causes rapidly increasing cell death as the dose is raised, with viability down to 40% at the highest dose. The trends with both K237-CS(PTX)-g-PNIPAM and CS(PTX)-g-PNIPAM are similar: viability decreases markedly as the PTX concentration is raised. The results with CS(PTX)-g-PNIPAM are essentially identical to those with free PTX at all doses. In contrast, however, K237-CS(PTX)-g-PNIPAM causes more cell death than free PTX throughout. This is particularly marked at 10 µg/mL, where the viability with K237-CS(PTX)-g-PNIPAM (at 20%) is half that of PTX alone [51, 52]. It thus appears that the K237 functionalization enables the NP's drug cargo to be more effectively delivered to cancer cells. This suggests that these novel materials may be highly effective chemotherapeutic drug carriers that can alleviate the unpleasant side effects typically caused by the non-selectivity of such treatments.

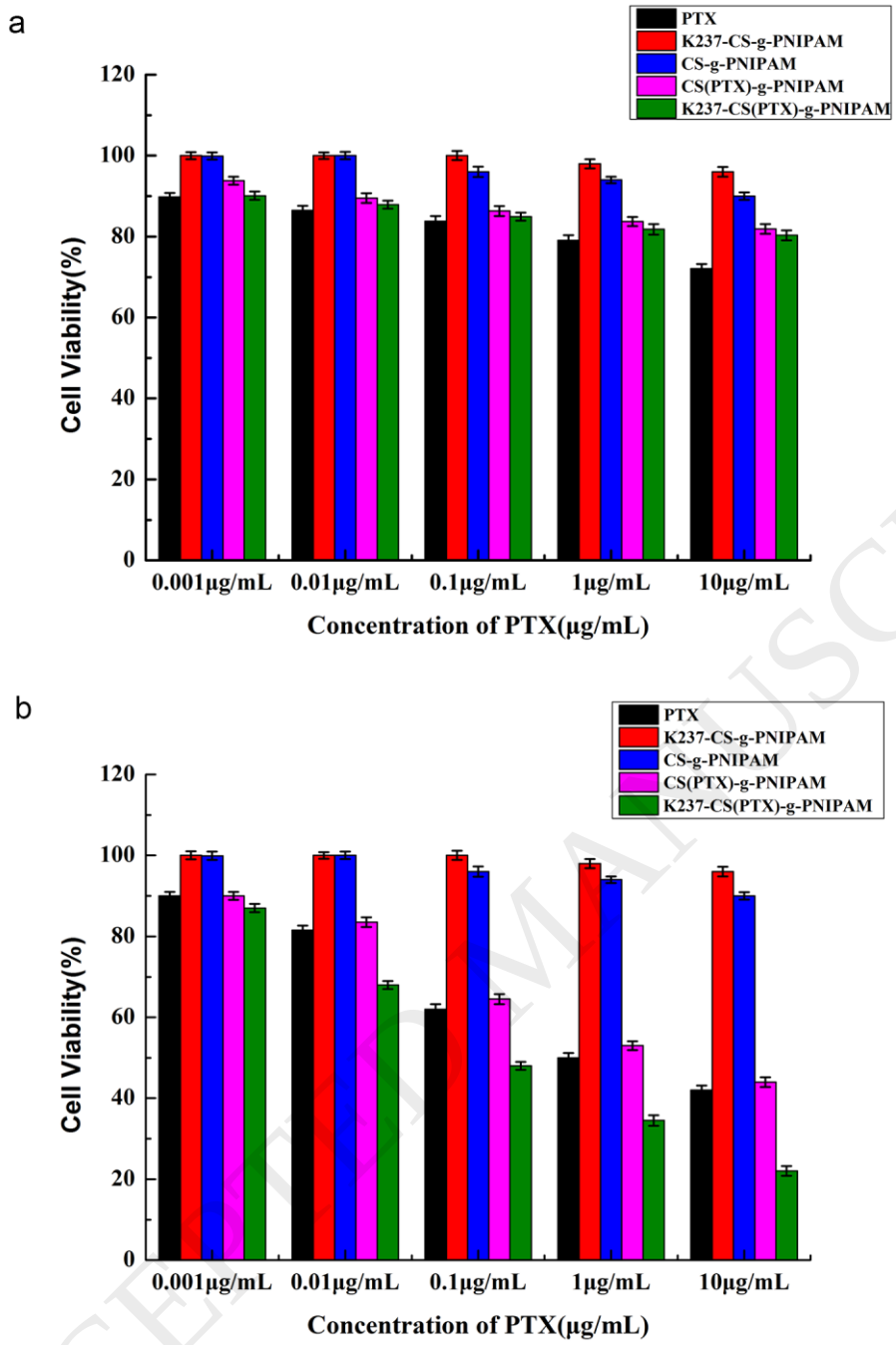

Fig. 6 The results of MTT viability assays of **a** L929 cells and **b** MDA-MB-231 cells treated with free PTX, drug-free K237-CS-g-PNIPAM and CS-g-PNIPAM, and drug-loaded K237-CS(PTX)-g-PNIPAM and CS(PTX)-g-PNIPAM at PTX concentrations of 0.001–10μg/mL. Analyses were conducted after 24 h incubation. Data are reported as mean ± SD.

To obtain more information on the mechanism of action of the K237-functionalized NPs, K237-CS-g-PNIPAM and CS-g-PNIPAM were labelled with FITC. L929 and MDA-MB-231 cells were then treated with FITC-labelled CS(PTX)-g-PNIPAM and K237-CS(PTX)-g-PNIPAM, and the cells were examined by confocal laser scanning microscopy. The results are given in Fig. 7. The cell nuclei are

stained blue (Hoechst), with the FITC-labelled formulations fluorescing green [53]. The images clearly show that MBA-MD-321 cells exhibit a greater amount of uptake of K237-CS(PTX)-g-PNIPAM than of CS(PTX)-g-PNIPAM, with a higher intracellular fluorescence signal in the former case. Uptake is much reduced in the case of the L929 cells, and there was no difference between those treated with CS (PTX)-g-PNIPAM and K237-CS (PTX)-g-PNIPAM. These data indicate the conjugated K237 could facilitate the internalization of NPs in MAD-MB-231 cells. This is because the K237 peptide is able to bind to KDR / Flk-1 tyrosine kinase, one of the two receptors of vascular endothelial growth factor overexpressed on tumor neovascularization (and on MAD-MB-231 cells), with high affinity and specificity, promoting the uptake of the functionalized CS material [54]. These results demonstrate that K237-CS (PTX)-g-PNIPAM can actively target MDA-MB-231 cells, allowing the loaded drug to be delivered specifically to the tumor site.

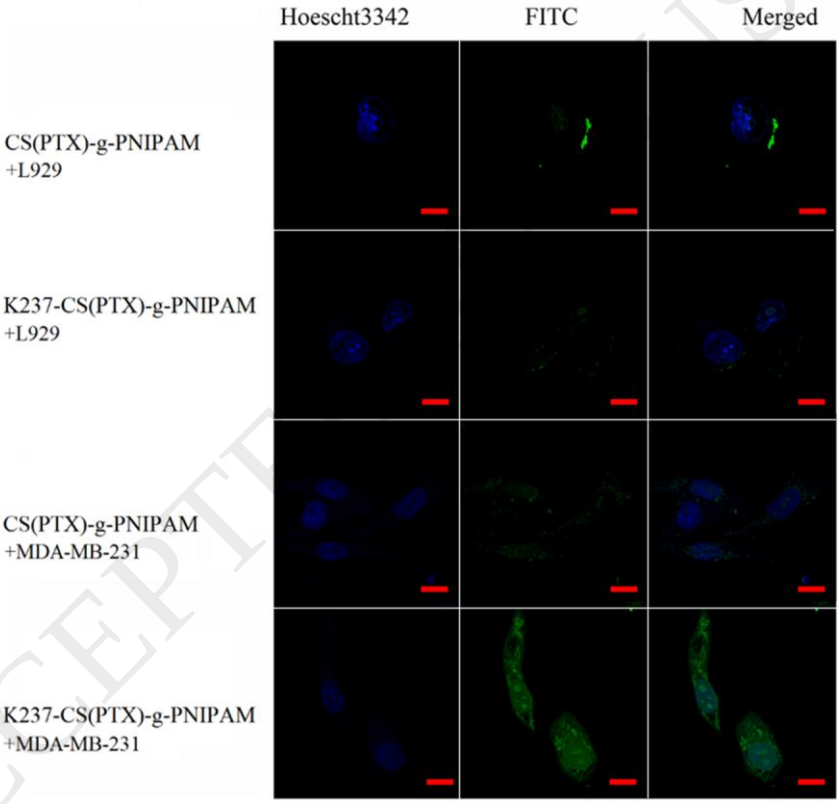

Fig. 7 Confocal microscopy images of MDA-MB-231 and L929 cells treated with CS (PTX)-g-PNIPAM –PTX NPs or K237-CS (PTX)-g-PNIPAM NPs for 2h. The scale bar represents 25 μm.

4. Conclusions

A novel anticancer drug delivery system based on CS has been developed to provide targeted delivery to breast cancer cells. CS was sensitive to pH, grafting the thermosensitive polymer PNIPAM to generate dual temperature and pH-responsive CS NPs of around 100 nm in size. The copolymers

were then conjugated with a breast cancer targeting peptide (K237) and the anticancer drug paclitaxel (PTX) was loaded into the system. In the mildly acidic pH typical of the tumor microenvironment, PTX was released more rapidly than under normal physiological conditions. Higher temperatures also accelerated PTX release. In *vitro* studies showed that the CS-based NPs have good biocompatibility. In addition, K237-conjugated NPs were internalized to a greater extent in tumor cells, and are much more toxic to cancerous than non-cancerous cells. This is thought to occur due to the selective recognition of K237 by the KDR/Flk 1 tyrosine kinase receptors which are over-expressed on breast cancer cells. Overall, the K237-CS (PTX)-g-PNIPAM NPs system prepared in this work appears to have great potential for targeted cancer therapy.

Acknowledgements

This work was supported by the Science and Technology Commission of Shanghai Municipality (grant 16410723700); Biomedical Textile Materials “111Project” from Ministry of Education of China (No.B07024); the National Natural Scientific Foundation of China (No.81460647) and the UK-CHINA Joint Laboratory for Therapeutic Texiles.

References

[1] J. Ferlay, H.R. Shin, F. Bray, D. Forman, C. Mathers, D.M. Parkin, Estimates of worldwide burden of cancer in 2008: GLOBOCAN 2008, Int. J. Cancer 127 (2010) 2893-2917.

[2] C. Desantis, J. Ma, L. Bryan, A. Jemal, Breast cancer statistics, 2013, Ca. Cancer J. Clin. 64 (2014) 52-62.

[3] Z. Zhang, L. Mei, S.S. Feng, Paclitaxel drug delivery systems, Expert Opin. Drug Del. 10 (2013) 325-340.

[4] Z.W. Jing, Y.Y. Jia, N. Wan, M. Luo, M.L. Huan, T.B. Kang, S.Y. Zhou, B.L. Zhang, Design and evaluation of novel pH-sensitive ureido-conjugated chitosan/TPP nanoparticles targeted to Helicobacter pylori, Biomaterials 84 (2016) 276-285.

[5] J.P. Nam, S.C. Park, T.H. Kim, J.Y. Jang, C. Choi, M.K. Jang, J.W. Nah, Encapsulation of paclitaxel into lauric acid-O-carboxymethyl chitosan-transferrin micelles for hydrophobic drug delivery and site-specific targeted delivery, Int. J. Pharm. 457 (2013) 124-135.

[6] X. Zhang, H. Zhang, L. Yin, R. Hu, T. Qiu, Y. Yin, X. Xiong, H. Zheng, Q. Wang, A pH-Sensitive Nanosystem Based on Carboxymethyl Chitosan for Tumor-Targeted Delivery of Daunorubicin, J. Biomed. Nanotechnol. 12 (2016) 1688-1698.

[7] T. Lammers, F. Kiessling, W.E. Hennink, G. Storm, Drug targeting to tumors: Principles, pitfalls and (pre-) clinical progress, J. Control. Release 161 (2012) 175-187.

[8] R. Palumbo, F. Sottotetti, A. Bernardo, Targeted chemotherapy with nanoparticle albumin-bound paclitaxel (nab-paclitaxel) in metastatic breast cancer: which benefit for which patients?, Ther. Adv. Med. Oncol. 8 (2016) 209-229.

[9] S.V. Talluri, G. Kuppusamy, S. Tummala, S.R.V. Madhunapantula, Lipid-based nanocarriers for breast cancer treatment – comprehensive review, Drug Deliv. 23 (2016) 1291-1305.

[10] T.M. Allen, P.R. Cullis, Liposomal drug delivery systems: from concept to clinical applications, Adv. Drug Deliv. Rev. 65 (2013) 36-48.

[11] Q. Feng, Y. Zhang, W. Zhang, X. Shan, Y. Yuan, H. Zhang, L. Hou, Z. Zhang, Tumor-targeted and multi-stimuli responsive drug delivery system for near-infrared light induced chemo-phototherapy and photoacoustic tomography, Acta Biomater. 38 (2016) 129-142.

[12] E. Piktel, K. Niemirowicz, M. Wątek, T. Wollny, P. Deptuła, R. Bucki, Recent insights in nanotechnology-based drugs and formulations designed for effective anti-cancer therapy, J. Nanobiotechnol. 14 (2016) 39-61.

[13] d.Z.J. Van, Heating the patient: a promising approach?, Ann. Oncol. 13 (2002) 1173-1184.

[14] H. Yang, D.H. Bremner, L. Tao, H. Li, J. Hu, L. Zhu, Carboxymethyl chitosan-mediated synthesis of hyaluronic acid-targeted graphene oxide for cancer drug delivery, Carbohydr. Polym. 135 (2016) 72-78.

[15] V.P. Torchilin, Multifunctional, stimuli-sensitive nanoparticulate systems for drug delivery, Nat. Rev. Drug Discov. 13 (2014) 813-827.

[16] S. Niu, D.H. Bremner, J. Wu, J. Wu, H. Wang, H. Li, Q. Qian, H. Zheng, L. Zhu, l-Peptide functionalized dual-responsive nanoparticles for controlled paclitaxel release and enhanced apoptosis in breast cancer cells, Drug Deliv. 25(2018) 1275-1288

[17] T. Kean, M. Thanou, Biodegradation, biodistribution and toxicity of chitosan, Adv. Drug Deliv. Rev. 62 (2010) 3-11.

[18] M. Kumar, M. Kumar, N. Majeti, M.N.V. Ravi Kumar, R.A.A. Muzzarelli, C. Muzzarelli, H.

Sashiwa, A.J. Domb, Review: A review of chitin and chitosan applications, Chem. Rev. 36 (2000) 6017-6084.

[19] A.M. De Campos, A. Sánchez, M.J. Alonso, Chitosan nanoparticles: a new vehicle for the improvement of the delivery of drugs to the ocular surface. Application to cyclosporin A, Int. J. Pharm. 224 (2001) 159-168.

[20] K. Nagpal, S.K. Singh, D.N. Mishra, Chitosan nanoparticles: a promising system in novel drug delivery, Chem. Pharm. Bull. 58 (2010) 1423-1430.

[21] M. Constantin, S.M. Bucatariu, F. Doroftei, G. Fundueanu, Smart composite materials based on chitosan microspheres embedded in thermosensitive hydrogel for controlled delivery of drugs, Carbohydr. Polym. 157 (2017) 493-502.

[22] J. Jiang, D. Hua, J. Tang, One-pot synthesis of pH- and thermo-sensitive chitosan-based nanoparticles by the polymerization of acrylic acid/chitosan with macro-RAFT agent, Int. J. Biol. Macromol. 46 (2010) 126-130.

[23] R. Szm, Z. Ahmad, A. Khan, H.M. Akil, O. Mbh, H. Zaa, F. Ullah, Synthesis and evaluation on pH- and temperature-responsive chitosan-p(MAA-co-NIPAM) hydrogels, Int. J. Biol. Macromol. 108 (2017) 367-375.

[24] T. Yadavalli, S. Ramasamy, G. Chandrasekaran, I. Michael, H.A. Therese, R. Chennakesavulu, Dual responsive PNIPAM–chitosan targeted magnetic nanopolymers for targeted drug delivery, J. Magn. Magn. Mater. 380 (2015) 315-320.

[25] J. Tang, D. Hua, J. Cheng, J. Jiang, X. Zhu, Synthesis and properties of temperature-responsive chitosan by controlled free radical polymerization with chitosan-RAFT agent, Int. J. Biol. Macromol. 43 (2008) 383-389.

[26] M. Srinivasarao, C.V. Galliford, P.S. Low, Principles in the design of ligand-targeted cancer therapeutics and imaging agents, Nat. Rev. Drug Discov. 14 (2015) 203-219.

[27] A. Saneja, D. Arora, R. Kumar, R.D. Dubey, A.K. Panda, P.N. Gupta, CD44 targeted PLGA nanomedicines for cancer chemotherapy, Eur. J. Pharm. Sci. 121 (2018) 47-58.

[28] D.K. Prusty, V. Adam, R.M. Zadegan, S. Irsen, M. Famulok, Supramolecular aptamer nano-constructs for receptor-mediated targeting and light-triggered release of chemotherapeutics into cancer cells, Nat. Commun. 9 (2018) 535-548.

[29] S.D. Yang, W.J. Zhu, Q.L. Zhu, W.L. Chen, Z.X. Ren, F. Li, Z.Q. Yuan, J.Z. Li, Y. Liu, X.F. Zhou, Binary-copolymer system base on low-density lipoprotein-coupled N-succinyl chitosan lipoic acid micelles for co-delivery MDR1 siRNA and paclitaxel, enhances antitumor effects via reducing drug, J. Biomed. Mater. Res. Part B 105 (2017) 1114-1125.

[30] L. Shan, X. Zhuo, F. Zhang, Y. Dai, G. Zhu, B.C. Yung, W. Fan, K. Zhai, O. Jacobson, D.O. Kiesewetter, A paclitaxel prodrug with bifunctional folate and albumin binding moieties for both passive and active targeted cancer therapy, Theranostics 8 (2018) 2018-2030.

[31] N. Rizk, N. Christoforou, S. Lee, Optimization of anti-cancer drugs and a targeting molecule on multifunctional gold nanoparticles, Nanotechnology 27 (2016) 185704.

[32] Y. Zhong, K. Goltsche, L. Cheng, F. Xie, F. Meng, C. Deng, Z. Zhong, R. Haag, Hyaluronic acid-shelled acid-activatable paclitaxel prodrug micelles effectively target and treat CD44-overexpressing human breast tumor xenografts in vivo, Biomaterials 84 (2016) 250-261.

[33] M. Talelli, M. Iman, C.J. Rijcken, C.F. van Nostrum, W.E. Hennink, Targeted core-crosslinked polymeric micelles with controlled release of covalently entrapped doxorubicin, J. Control. Release 31 (2010) 7797-7804.

[34] J. Yao, J. Feng, X. Gao, D. Wei, T. Kang, Q. Zhu, T. Jiang, X. Wei, J. Chen, Neovasculature and circulating tumor cells dual-targeting nanoparticles for the treatment of the highly-invasive breast cancer, Biomaterials 113 (2016) 1-17.

[35] S.H. Wang, C.L. Lee, I.J. Chen, N.C. Chang, H.C. Wu, H.M. Yu, Y.J. Chang, T.W. Lee, J.C. Yu, A.L. Yu, Structure-based optimization of GRP78-binding peptides that enhances efficacy in cancer imaging and therapy, Biomaterials 94 (2016) 31-44.

[36] T. Dai, L. Na, F. Han, Z. Hua, Y. Zhang, L. Qin, AMP-guided tumour-specific nanoparticle delivery via adenosine A 1 receptor, Biomaterials 83 (2016) 37-50.

[37] L. Fan, Y. Zhang, F. Wang, Q. Yang, J. Tan, G. Renata, H. Wu, C. Song, B. Jin, Multifunctional all-in-one drug delivery systems for tumor targeting and sequential release of three different anti-tumor drugs, Biomaterials 76 (2016) 399-407.

[38] Y. Zhou, S. Hua, J. Yu, P. Dong, F. Liu, D. Hua, A strategy for effective radioprotection by chitosan-based long-circulating nanocarriers, J. Mater. Chem. B 3 (2015) 2931-2934.

[39] Q. Pan, Y. Lv, G.R. Williams, L. Tao, H. Yang, H. Li, L. Zhu, Lactobionic acid and carboxymethyl chitosan functionalized graphene oxide nanocomposites as targeted anticancer drug delivery systems, Carbohydr. Polym. 151 (2016) 812-820.

[40] D. Hua, J. Tang, J. Cheng, W. Deng, X. Zhu, A novel method of controlled grafting modification of chitosan via RAFT polymerization using chitosan-RAFT agent, Carbohydr. Polym. 73 (2008) 98-104.

[41] S. Hua, J. Yu, J. Shang, H. Zhang, J. Du, Y. Zhang, F. Chen, Y. Zhou, F. Liu, Effective tumor-targeted delivery of etoposide using chitosan nanoparticles conjugated with folic acid and sulfobetaine methacrylate, Rsc Adv. 6 (2016) 91192-91200.

[42] Y. Wang, H. Xu, J. Wang, L. Ge, J. Zhu, Development of a thermally responsive nanogel based on chitosan-poly(N-isopropylacrylamide-co-acrylamide) for paclitaxel delivery, J. Pharm. Sci. 103 (2014) 2012–2021.

[43] Y. Wang, J. Wang, Z. Yuan, H. Han, T. Li, L. Li, X. Guo, Chitosan cross-linked poly(acrylic acid) hydrogels: Drug release control and mechanism, Colloid. Surface. B 152 (2017) 252-259.

[44] F. Ming, M. Ye, H. Tan, J. Yang, S. Zou, S. Guo, Z. Meng, H. Hao, Z. Ling, C. Yong, Covalent and injectable chitosan-chondroitin sulfate hydrogels embedded with chitosan microspheres for drug delivery and tissue engineering, Mater. Sci. Eng. C 71 (2017) 67-74.

[45] M. Roldo, D.G. Fatouros, Chitosan-Derivative Based Hydrogels as Drug Delivery Platforms: Applications in Drug Delivery and Tissue Engineering, Springer Berlin Heidelberg 8 (2011) 351-376.

[46] S. Huang, K. Shao, Y. Liu, Y. Kuang, J. Li, S. An, Y. Guo, H. Ma, C. Jiang, Tumor-targeting and microenvironment-responsive smart nanoparticles for combination therapy of antiangiogenesis and apoptosis, Acs Nano 7 (2013) 2860-2871.

[47] R. Matsumoto, M. Okochi, K. Shimizu, K. Kanie, R. Kato, H. Honda, Effects of the properties of short peptides conjugated with cell-penetrating peptides on their internalization into cells, Sci. Rep. 5 (2015) 12884.

[48] Z. Wang, W.K. Chui, Nanoparticulate delivery system targeted to tumor neovasculature for combined anticancer and antiangiogenesis therapy, Pharm. Res. 28 (2011) 585-596.

[49] P.B. Kajjari, L.S. Manjeshwar, T.M. Aminabhavi, Novel Interpenetrating Polymer Network Hydrogel Microspheres of Chitosan and Poly(acrylamide)-grafted-Guar Gum for Controlled Release of Ciprofloxacin, Ind. Eng. Chem. Res. 50 (2011) 13280-13287.

[50] GANGULY, Kuntal, AMINABHAVI, M. Tejraj, KULKARNI, R. Anandrao, Colon Targeting of 5-Fluorouracil Using Polyethylene Glycol Cross-linked Chitosan Microspheres Enteric Coated with Cellulose Acetate Phthalate, Ind. Eng. Chem. Res. 50 (2011) 11797-11807.

[51] L. Mercurio, M.A. Ajmone-Cat, S. Cecchetti, A. Ricci, G. Bozzuto, A. Molinari, I. Manni, B. Pollo, S. Scala, G. Carpinelli, Targeting CXCR4 by a selective peptide antagonist modulates tumor microenvironment and microglia reactivity in a human glioblastoma model, J. Exp. Clin. Cancer Res. 35 (2016) 55-69.

[52] Q. Song, Y. Yin, L. Shang, T. Wu, D. Zhang, M. Kong, Y. Zhao, Y. He, S. Tan, Y. Guo, Tumor Microenvironment Responsive Nanogel for the Combinatorial Antitumor Effect of Chemotherapy and Immunotherapy, Nano Lett. 17 (2017) 6366-6375.

[53] W.J. Zhu, S.D. Yang, C.X. Qu, Q.L. Zhu, W.L. Chen, F. Li, Z.Q. Yuan, Y. Liu, B.G. You, X.N. Zhang, Low-density lipoprotein-coupled micelles with reduction and pH dual sensitivity for intelligent co-delivery of paclitaxel and siRNA to breast tumor, Int. J. Nanomed. 12 (2017) 3375-3393.

[54] F. Jin, Z. Xie, C.J. Kuo, L.W. Chung, C.L. Hsieh, Cotargeting tumor and tumor endothelium effectively inhibits the growth of human prostate cancer in adenovirus-mediated antiangiogenesis and oncolysis combination therapy, Cancer Gene Ther. 12 (2005) 257-267.